

Supplementary Information

Surface energy and wettability of van der Waals structures

Meenakshi Annamalai^a, Kalon Gopinadhan^{*a,b}, Sang A Han^{c,d}, Surajit Saha^{a,e}, Hye Jeong Park^c, Brijesh Kumar^{#a}, Abhijeet Patra^{a,f}, Sang-Woo Kim^{*c,d}, T Venkatesan^{*a,b,e,f,g}

^aNUSNNI-NanoCore, National University of Singapore (NUS), Singapore 117411

^bDepartment of Electrical and Computer Engineering, National University of Singapore (NUS), Singapore 117583

^cNanoelectronic Science and Engineering Laboratory, Department of Advanced Materials Science & Engineering, School of Engineering, Sungkyunkwan University, Suwon 440-746, Republic of Korea

^dSKKU Advanced Institute of Nanotechnology (SAINT), Center for Human Interface Nanotechnology (HINT), Sungkyunkwan University, Suwon 440-746, Republic of Korea

^eDepartment of Physics, Faculty of Science, National University of Singapore (NUS), Singapore 117551

^fNUS Graduate School for Integrative Sciences and Engineering (NGS), National University of Singapore (NUS), Singapore 117456

^gDepartment of Materials Science and Engineering, National University of Singapore (NUS), Singapore 117575

[#]Currently at Centre for Nanoscience and Technology, School of Engineering and Technology, Amity University, Gurgaon 122413, India

Corresponding author Email: venky@nus.edu.sg; kimsw1@skku.edu;
gopinadhan@iitkalumni.org

Macroscale contact angle and surface energy measurement

Wettability of surfaces by liquids is of great interest in a number of fields ranging from engineering to medicine. Wetting phenomena on a macroscopic scale can be illustrated using Young's equation.¹

$$\gamma_{lv}\cos\theta = \gamma_{sv} - \gamma_{sl} \quad (1)$$

where θ is the contact angle, γ_{sl} is solid/liquid interfacial free energy, γ_{lv} is liquid/vapour interfacial tension (liquid surface tension) and γ_{sv} solid surface free energy.

The contact angle is estimated using the sessile drop technique by measuring the angle between the tangent lines along solid-liquid interface and liquid-vapour interface of the liquid contour as shown in Fig. S1. A contact angle of 0° and 180° correspond to complete wetting and non-wetting respectively. Surfaces exhibiting contact angles below 90° are called hydrophilic and those above 90° are called hydrophobic. In the past few decades many semi-empirical analytical models have been developed to compute surface free energy from measured contact angles such as Fowkes,² Owens Wendt Rabel and Kaelbel (OWRK),³ Van Oss-Chaudhury Good/Lewis acid base theory,⁴ Zisman⁵ and Neumann,⁶ to name a few. Each approach is targeted for measuring surface energies of either low surface energy materials or high surface materials or both. Also, the essence and physical interpretation of these approaches are different and therefore subsequently provide information on total surface energy or individual components (polar, dispersive, hydrogen bonding etc.) of surface energy or both. In our work, the OWRK method has been adopted which is suitable for universal systems.

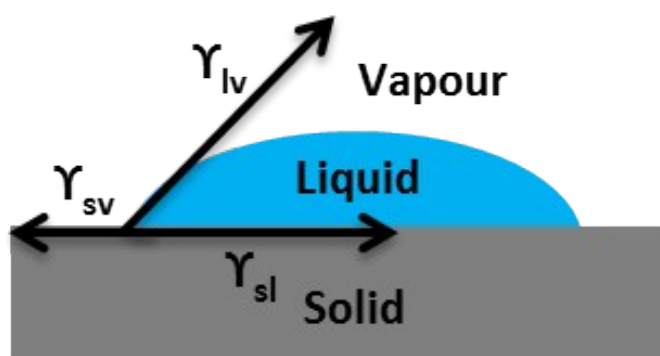


Figure S1. Schematic diagram of a liquid drop on a solid surface showing the interfacial tensions at three phase boundary.

Description of OWRK method

Owens, Wendt, Rabel and Kaelble developed a two component model to separate the interfacial tension according to the underlying interactions between the molecules. These interactions are defined as polar and dispersive interactions. The total surface energy of the solid is the sum of the two parts. The polar interactions arise due to the permanent dipole – permanent dipole interactions or Keesom forces.⁷ They are stronger and only exist in polar molecules. Dispersive component also known as London forces are weak and arise due to

random fluctuations in the electron density in an electron cloud and hence lead to temporary/induced dipole interactions.⁸

In OWRK method, at least two liquids with known dispersive and polar parts of surface tensions are needed to compute the solid surface free energy as there are two unknowns (solid/liquid interfacial free energy and solid surface free energy). The combining rule proposed by OWRK model is indicated below.

$$\gamma_{sl} = \gamma_{sv} + \gamma_{lv} - 2\left(\sqrt{\gamma_{sv}^D \gamma_{lv}^D} + \sqrt{\gamma_{sv}^P \gamma_{lv}^P}\right) \quad (2)$$

Where γ_{sv}^D and γ_{lv}^D are dispersive components and γ_{sv}^P and γ_{lv}^P are polar components of solid and liquid surface energies respectively.

Substituting for γ_{sl} from equation (1),

$$\sqrt{\gamma_{sv}^D \gamma_{lv}^D} + \sqrt{\gamma_{sv}^P \gamma_{lv}^P} = \frac{1}{2}[\gamma_{sv} + \gamma_{lv} - (\gamma_{sv} - \gamma_{lv} \cos\theta)] \quad (3)$$

$$\sqrt{\gamma_{sv}^D \gamma_{lv}^D} + \sqrt{\gamma_{sv}^P \gamma_{lv}^P} = \frac{1}{2}[\gamma_{lv}(1 + \cos\theta)] \quad (4)$$

By dividing $\sqrt{\gamma_{lv}^D}$ in equation (4), we get,

$$\sqrt{\gamma_{sv}^D} + \sqrt{\gamma_{sv}^P} \frac{\sqrt{\gamma_{lv}^P}}{\sqrt{\gamma_{lv}^D}} = \frac{1}{2} \frac{[\gamma_{lv}(1 + \cos\theta)]}{\sqrt{\gamma_{lv}^D}} \quad (5)$$

The above equation can be represented in the linear form,

$$c + mx = y \quad (6)$$

where in, $c = \sqrt{\gamma_{sv}^D}$ $m = \sqrt{\gamma_{sv}^P}$ $x = \frac{\sqrt{\gamma_{lv}^P}}{\sqrt{\gamma_{lv}^D}}$

A graphical representation of the OWRK method is shown in Fig. S2 for MoS₂ on SiO₂-Si. The polar and dispersive components of total surface tension of the liquids used in this study are known (Table S1) and are substituted to compute the polar and dispersive components of the surface free energy of the solid. The slope of the graph gives the polar component and the vertical intercept gives the dispersive component of the solid surface free energy.

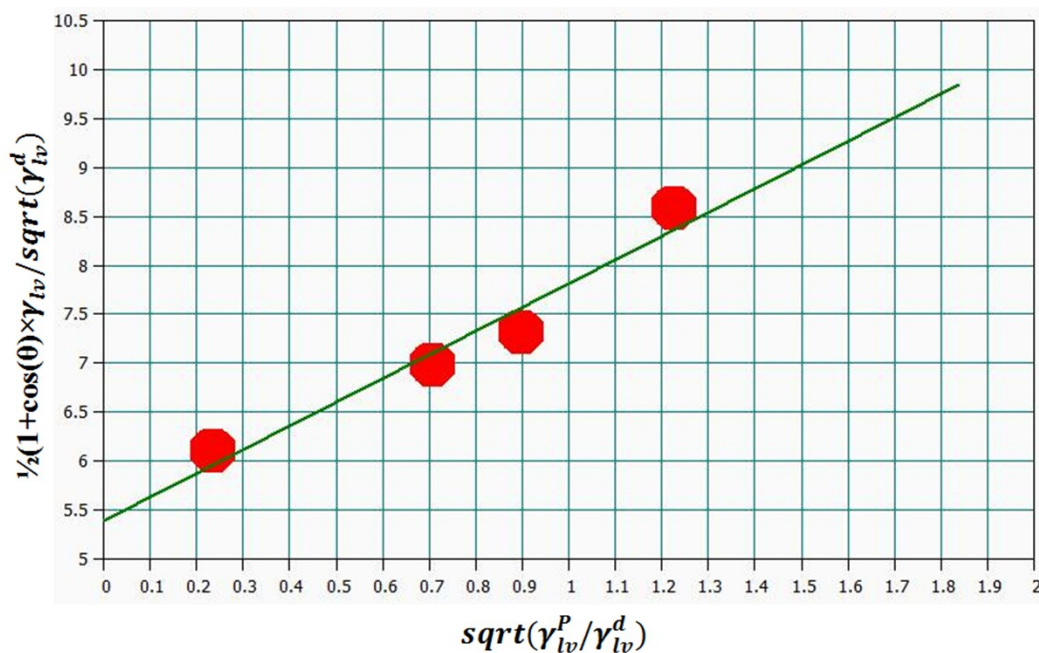


Figure S2. A representative surface energy (polar and dispersive) calculation graph based on OWRK model for MoS₂/SiO₂/Si sample.

Table S1. Surface tensions (SFT) of the test liquids

Solvent	SFT (Total) mN/m	SFT (Dispersive) mN/m	SFT (Polar) mN/m	Values Adapted From
Water	72.80	29.10	43.70	Chen <i>et al.</i>
Ethylene Glycol	47.70	26.40	21.30	Gebhardt <i>et al.</i>
Diiodomethane	50.00	47.40	2.60	Busscher <i>et al.</i>
Formamide	59.00	39.40	19.60	Rabel <i>et al.</i>

For determining the thickness of h-BN, h-BN has been transferred to a copper grid for TEM characterization. The high resolution TEM image on the edge of h-BN is shown Fig. S3. The image shows the crystalline and layered nature of h-BN where the number of BN layers is determined to be ~10.

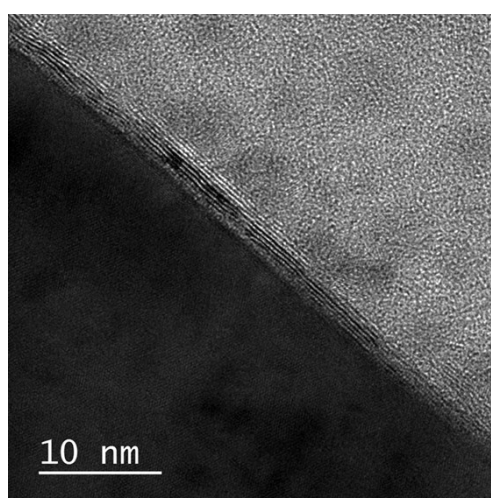


Figure S3. A transmission electron microscope (TEM) cross sectional image of h-BN.

Measured contact angles with four test liquids on the fabricated 2D structures are shown in Table S2. The standard deviation has been calculated based on the variations in the measured left and right contact angles and also taking in to account the instrumental uncertainty of 0.1°. Figure S4 shows the contact angle images obtained for ethylene glycol, diiodomethane and formamide on the 2D structures.

Table S2. Contact angles obtained from four different solvents on the fabricated surfaces

S/N	Sample Details	Water CA (degrees)	Water CA Repeat (degrees)	Ethylene Glycol CA (degrees)	Diiodomethane CA (degrees)	Formamide CA (degrees)
1	Graphene/h-BN/SiO ₂ /Si	79.1±0.2	78.4±0.4	51.1±0.6	44.3±0.5	61.5±0.3
2	MoS ₂ /h-BN/SiO ₂ /Si	61.6±0.2	60.6±0.2	39.3±0.2	35.1±0.3	56.6±0.6
3	WS ₂ /h-BN/SiO ₂ /Si	66.4±0.4	68.5±0.2	47.7±0.5	38.6±0.4	58.5±1.5
4	MoS ₂ /WS ₂ /h-BN/SiO ₂ /Si	63.3±0.4	60.7±0.2	44.1±0.2	31.1±0.1	53.6±0.4
5	Graphene/SiO ₂ /Si	86.3±0.2	84.6±0.8	59.5±0.9	49.3±0.2	65.6±0.3
6	MoS ₂ /SiO ₂ /Si	74.3±0.1	76.6±1.1	54.8±0.3	47.3±1.4	61.0±1.8
7	WS ₂ /SiO ₂ /Si	71.2±0.2	68.5±0.2	48.4±1	36.7±0.1	57.6±0.2
8	MoS ₂ /WS ₂ /SiO ₂ /Si	89.9±0.5	87.7±0.4	63.0±1	45.4±0.6	59.9±0.5

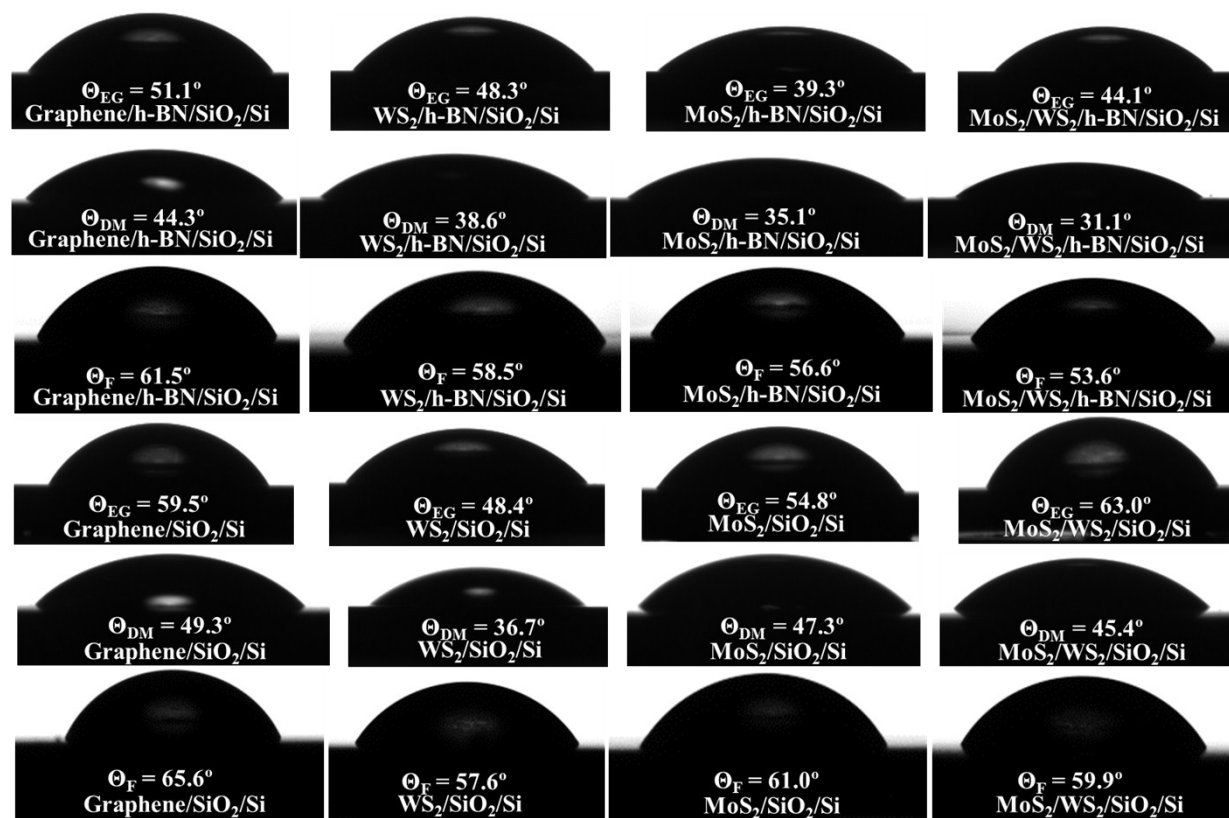


Figure S4. Contact angles obtained on various fabricated structures with ethylene glycol, diiodomethane and formamide.

From earlier reports on wetting of 2D materials we also believe that airborne contaminants have a pronounced impact on wettability and can significantly modify the water contact angle. The contact angle measurements were carried out in a controlled class 10,000 clean room with 45 % RH condition. Annealing was also performed in the same clean room environment and the samples were measured immediately after the samples were cooled down to room temperature. Surfaces are believed to adsorb hydrocarbons from ambient air and such adsorption reduces the surface energy and increases the hydrophobicity of the material. In order to study such an influence of time over the wettability, we performed water contact angle (WCA) measurements over time ($t = 0$ to 24 hours) on $\text{MoS}_2/\text{SiO}_2/\text{Si}$. For annealing, we followed the procedure adopted in electrical measurements. For example, annealing at 400 K recovers the intrinsic surface of graphene/BN system as evident from the zero charge neutrality point.⁹ The samples used in this study were thermally annealed at 150 °C to remove any aromatic hydrocarbons and moisture that might be present on the surface before the contact angle measurements and with the samples exposed to the controlled clean room environment and even with ageing the WCA seems to be almost constant (see Fig. S5).

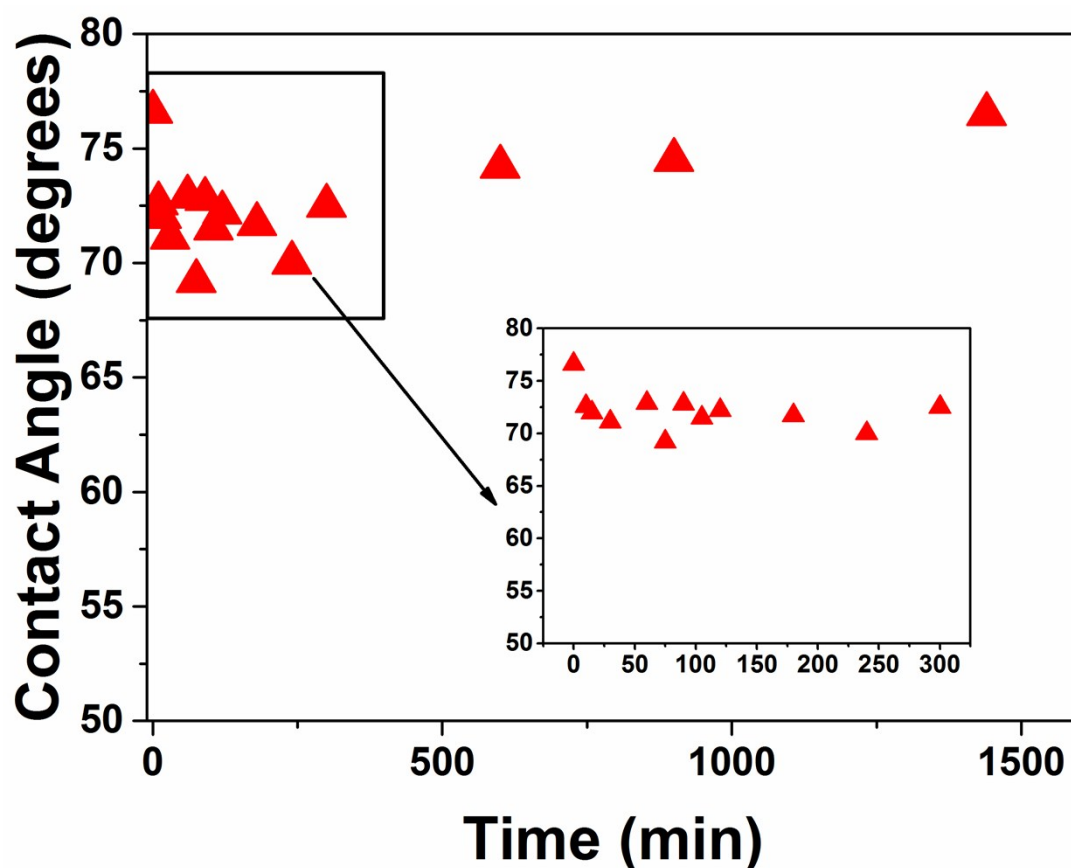


Figure S5. Water contact angle of $\text{MoS}_2/\text{SiO}_2/\text{Si}$ (thermally annealed at 150 °C) over time.

Any presence of MoO_3 should be reflected as a strong Raman peak at $\sim 820 \text{ cm}^{-1}$. A Raman spectrum of MoS_2 after 150 °C annealing showing absence of any peak near 820 cm^{-1} is shown in Fig. S6. So we can rule out the oxidation process at 150 °C.

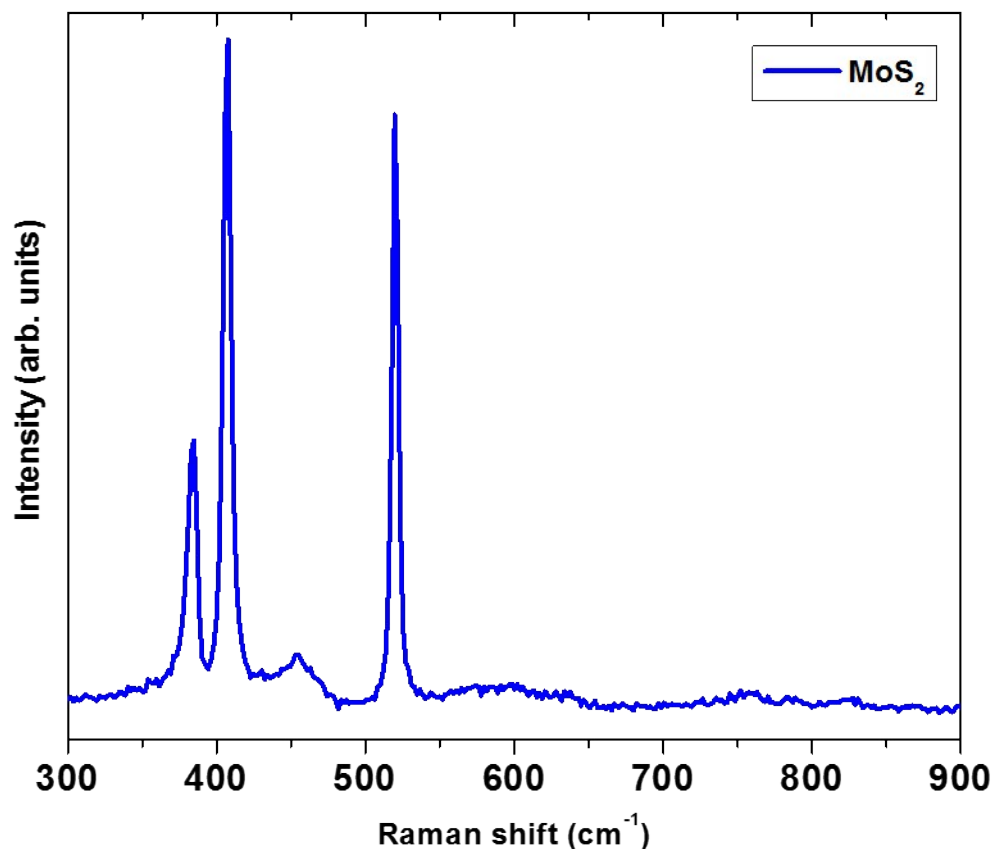


Figure S6. Raman spectrum of MoS₂ after 150 °C thermal annealing.

References

1. T. Young, *Phil. Trans. R. Soc. Lond.*, 1805, **95**, 65-87.
2. F. M. Fowkes, *J. Colloid Interface Sci.*, 1968, **28**, 493-505.
3. D. K. Owens and R. C. Wendt, *J. Appl. Polym. Sci.*, 1969, **13**, 1741-1747.
4. C. J. Van Oss, R. J. Good and M. K. Chaudhury, *J. Colloid Interface Sci.*, 1986, **111**, 378-390.
5. H. Fox and W. Zisman, *J. Colloid Sci.*, 1952, **7**, 109-121.
6. M. Zenkiewicz, *Polimery*, 2006, **51**, 584-587.
7. W. Keesom, *Proc. R. Acad. Amsterdam*, 1915.
8. F. London, *Trans. Faraday Soc.*, 1937, **33**, 8b-26.
9. D. A. Abanin, S. V. Morozov, L. A. Ponomarenko, R. V. Gorbachev, A. S. Mayorov, M. I. Katsnelson, K. Watanabe, T. Taniguchi, K. S. Novoselov, L. S. Levitov and A. K. Geim, *Science*, 2011, **332**, 328-330.